# Bulk Functionalization of Ethylene–Propylene Copolymers. IV. A Theoretical Approach

R. GRECO* and P. MUSTO

Istituto di Tecnologia dei Polimeri e Reologia del C.N.R., Via Toiano 6, 80072 Arco Felice, Napoli, Italy

SYNOPSIS

A theoretical model is developed for the bulk functionalization of ethylene–propylene copolymers on the basis of the molecular mechanism proposed in previous papers, with certain simplifying assumptions: (1) A steady state regime for all the radical species is hypothesized; (2) a number of termination reactions are neglected; (3) no monomer homopolymerization is allowed to occur. An analytical expression is derived in such a way. A comparison of the theoretical predictions with some experimental data, obtained varying the radical initiator concentration $[I]_0$ and the reaction temperature, $T$, shows satisfactory agreement at low values of $[I]_0$ and $T$. At higher values the molecular mechanism becomes more complex and the model is unable to fit the data.

## INTRODUCTION

Bulk functionalization of polyolefins has received considerable attention in recent years.[1-9] Polar groups such as maleic anhydride and esters have been grafted onto the polymer backbone in order to improve such properties as adhesion and dyeability or to perform successive reactions such as cross-linking or grafting. In our Institute a systematic investigation of this process has been carried out using ethylene–propylene copolymers (EPR) as polymeric substrate, dibutylmaleate (DBM) [R—OOC—CH=CH—COOR] as functionalizing molecule and bis($\alpha$-$\alpha$ dimethyl benzyl) peroxide (dicumyl peroxide, DCPO) as radical initiator. DBM was selected to be grafted onto the EPR chain on the basis of its low volatility, and especially of its compatibility with the polymeric substrate, and the DCPO was chosen considering its decomposition rate in the explored temperature range.

Several parameters which affect the kinetics of the reaction as well as its efficiency were investigated; in particular, the reaction temperature, the initial DCPO content and the composition and microstructure of the polymeric substrate. The experimental results were interpreted in terms of a proposed reaction mechanism.[5-7]

A crystal structural and superreticular investigation on the ethylene sequences of the functionalized rubber at different DBM grafting degrees yielded further insight into the complex molecular mechanism governing the process.[8] In the present paper we report on a simplified kinetic model based on the previously proposed reaction mechanism which attempts to quantitatively describe the observed kinetic behavior.

The comparison of the model predictions with the experimental results shows that the model can be successfully applied to the lower reaction temperatures and to the lower radical initiator concentrations in the investigated ranges. The implications of the failure of the proposed model in more extreme conditions are discussed in terms of the simplifying assumptions adopted in the model development.

## EXPERIMENTAL RESULTS

In a series of papers,[5-8] the bulk functionalization of EPR copolymers using DBM as the grafting model molecule and DCPO as the radical initiator has been investigated. The kinetics of the reaction was followed by Fourier transform IR spectroscopy (FTIR) and the degradation of the polymeric substrate was qualitatively monitored by solution viscometry.

* To whom correspondence should be addressed.

Journal of Applied Polymer Science, Vol. 44, 781–788 (1992)
 CCC 0021-8995/92/050781-08$04.00

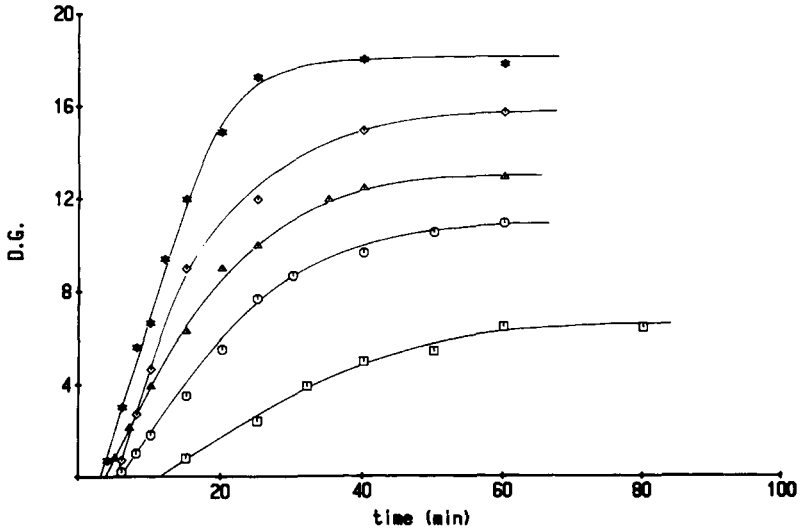


**Figure 1(a)** Influence of the DCPO concentration on the reaction kinetics: (□, ○, △, ◇, ★) refer to compositions A, B, C, D, and E of Table I, respectively. The reaction temperature is 150°C. The grafting degree is expressed as mmol of grafted DBM per 100 g of product.

Two sets of data were obtained on the same EPR copolymer by varying the reaction conditions as follows:

1. At a constant temperature (150°C) and at a fixed EPR/DBM ratio (100/10 parts by weight) the initial DCPO content of the reaction mixture was varied from 0.5 to 2.0 parts by weight. The results [see Fig. 1(a)] are consistent with an initial rate of grafting having a reaction order of one-half with respect to the radical initiator concentration $[I]_0$. An induction period was present for all the investigated compositions, where no DBM grafting was detectable by FTIR and where coupling reactions among polymeric macroradicals occurred as evidenced by viscosity measurements. The induction period was found to decrease by increasing $[I]_0$ whereas the rate of degradation followed an opposite trend. For the highest value of $[I]_0$ (2 parts by weight) a gradual increase of the

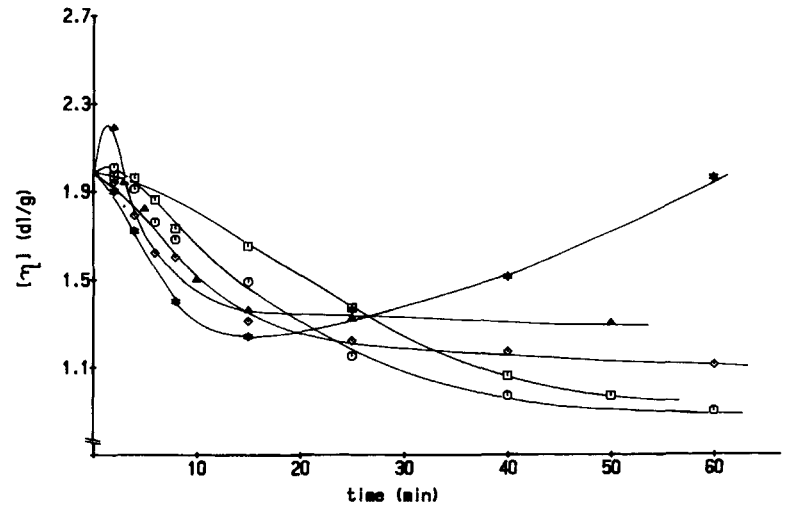


**Figure 1(b)** Dependence of the intrinsic viscosity of the products on the reaction time: (□, ○, △, ◇, ★) correspond to the reaction mixtures A, B, C, D, and E of Table I, respectively.

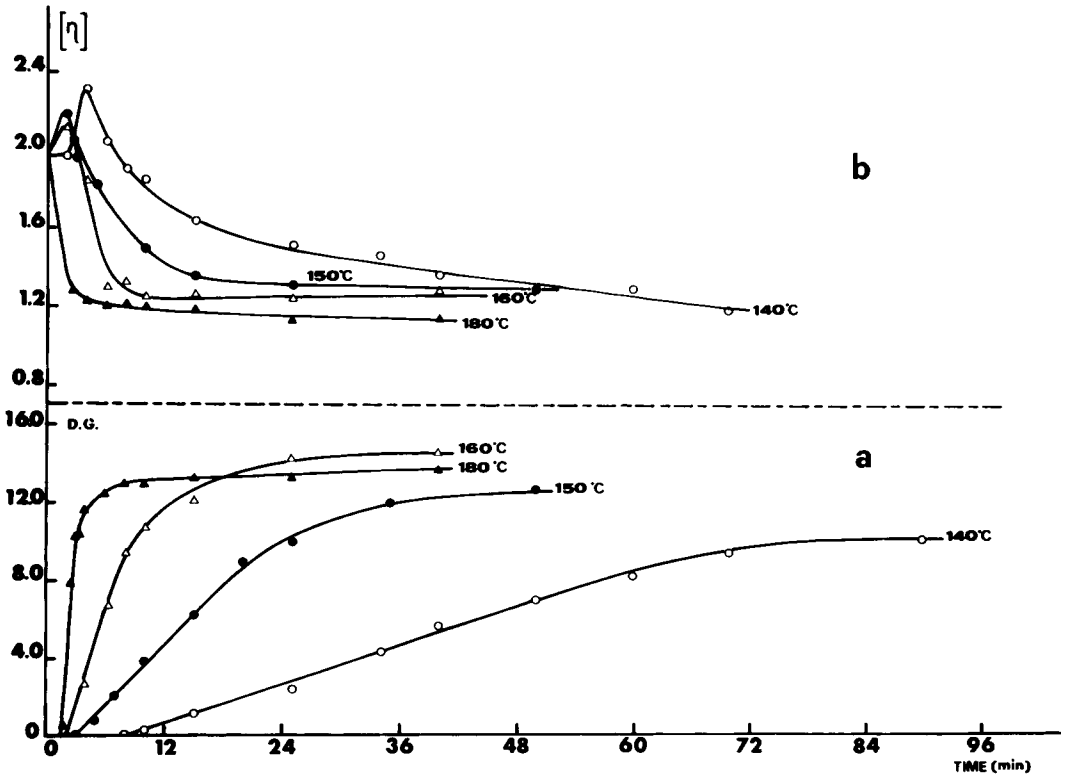


**Figure 2** Influence of the reaction time on the grafting degree (a) and on the intrinsic viscosity (b) for the reaction carried out at temperatures as indicated.

[$\eta$] values was observed at long reaction times, indicating an increase in molecular weight [see Fig. 1(b)].

2. At constant reactant composition (EPR/DBM/DCPO = 100/10/1) the temperature was varied from 130 up to 180°C. The initial rates of reaction showed a good correlation in an Arrhenius plot with an overall activation energy of 40 kcal/mol. Also in this case an induction period was observed whose length decreased by increasing the temperature (see Fig. 2).

## MODEL DEVELOPMENT

### Induction Period

A cage effect has been proposed to account for this phenomenon, due to the reduced molecular mobility of the polymeric substrate under the experimental conditions.[6,7] The reactions occurring therein can be summarized as follows:

$$I \xrightarrow{k_d} 2R\cdot \qquad \text{thermal decomposition of the radical initiator} \qquad (1)$$

$$R\cdot + PH \xrightarrow{k_i} P\cdot + RH \qquad \text{macroradical formation} \qquad (2)$$

$$P\cdot + P\cdot \xrightarrow{k_t} P{-}P \qquad \text{coupling reaction among macroradicals} \qquad (3)$$

Thus the net effect observed in the early stages of the process is an increase of the average molecular weight of the polymeric substrate. Other reactions can occur

$$P_1\cdot + P_2H \rightarrow P_2\cdot + P_1H \qquad \text{chain transfer} \qquad (4)$$

$$P\cdot \rightarrow P' + P''\cdot \qquad \beta\text{-scission reaction} \qquad (5)$$

$$P\cdot + R\cdot \rightarrow P{-}R \qquad \text{termination reaction} \qquad (6)$$

The relevance of reaction steps (4) and (5), which are minor in the early stages of the process, increases as the time elapses, thus producing a critical concentration of macroradicals in the system [step (4)], and an [$\eta$] decrease following the maximum observed in the induction period [step (5)]. For the

purpose of the present paper, one can conclude that the induction period has the following effects:

i. reduces by a certain amount the initial DCPO concentration $[I]_0$, by consuming primary radicals R· for reactions other than the DBM grafting;
ii. induces a complex molecular rearrangement of the EPR;
iii. builds up a critical concentration of various radical species.

## EPR Functionalization

The reaction steps occurring during the grafting process are the following:

$$P\cdot + M \xrightarrow{k_i} PM\cdot \quad \text{formation of PM macroradicals} \quad (7)$$

$$PM\cdot + PH \xrightarrow{k_p} P\cdot + PM \quad \text{transfer and product formation} \quad (8)$$

$$PM\cdot + M \rightarrow PMM\cdot \quad \text{monomer homopolymerization} \quad (9)$$

$$P\cdot + PM\cdot \rightarrow \text{inactive species} \quad \text{various termination reactions} \quad (10)$$

$$R\cdot + PM\cdot \rightarrow \text{inactive species} \quad (11)$$

$$PM\cdot + PM\cdot \rightarrow \text{inactive species} \quad (12)$$

In steps (10), (11), and (12) the termination reactions can occur either by macroradical coupling or by macroradical disproportionation.

For example, in step (10) we may have

$$P\text{—}PM \leftarrow P\cdot + PM\cdot \rightarrow PM + \diagup\!\!\diagdown$$

(coupling) (disproportionation)

In our model we will neglect step (9) because, since DBM is a 1,2-disubstituted olefin, it has a very limited tendency to homopolymerize.[5,6] Furthermore, by assuming an equal reactivity toward DBM addition of all the macroradical species generated, steps (4) and (5) can be neglected in our model.

Termination steps (10), (11), and (12) will not be considered, due to the low concentration of the radical species PM· in the system. Thus the only termination reaction which will be taken into account, is the one involving two P· macroradicals [step (3)]. It is worth noting that the relevance of the termination involving the species P· and R· [step (6)] depends on their concentration, that is, on $[I]_0$ and on temperature $T$, which in turn determines the decomposition rate of the radical initiator; this step can be neglected only as a first approximation.

In summary, we assume that the mechanism of the grafting reaction consists of the following steps:

$$I \xrightarrow{k_d} 2R\cdot$$

$$R\cdot + PH \xrightarrow{k_i} P\cdot + RH$$

$$P\cdot + M \xrightarrow{k_i'} PM\cdot$$

$$PM\cdot + PH \xrightarrow{k_p} PM + P\cdot$$

$$P\cdot + P\cdot \xrightarrow{k_t} \text{inactive species}$$

Step (5) ($\beta$-scission mechanism) has been neglected with respect to the DBM grafting reaction since no variation of the number of macroradicals is yielded by this step.

The rate of formation of the reaction product can be expressed by

$$\frac{d[PM]}{dt} = k_p[PM\cdot][PH] \quad (13)$$

To eliminate the unknown $[PM\cdot]$, it is possible to make a steady state assumption with respect to all the radical species present in the system. In other words, the concentration of these species is built up during the induction period to a steady-state negligible value, since they are consumed as soon as they are formed, with no possible accumulation.

This condition, applied to R·, P·, and PM· is expressed as follows:

$$\frac{d[R\cdot]}{dt} = 2k_d[I] - k_i[R\cdot][PH] = 0 \quad (14a)$$

$$\frac{d[P\cdot]}{dt} = k_i[R\cdot][PH] + k_p[PM\cdot][PH] - k_i'[P\cdot][M] - k_t[P\cdot]^2 = 0 \quad (14b)$$

$$\frac{d[PM\cdot]}{dt} = k_i'[P\cdot][M] - k_p[PM\cdot][PH] = 0 \quad (14c)$$

Summing all eqs. (14), one obtains

$$2k_d[I] - k_t[P\cdot]^2 = 0 \quad (15)$$

Therefore,

$$[P\cdot] = \left(\frac{2k_d[I]}{k_t}\right)^{1/2} \tag{16}$$

which is substituted in eq. (14c) to get [PM·]:

$$[PM\cdot] = \frac{k_i'[P\cdot][M]}{k_p[PH]} = \frac{k_i'[M]}{k_p[PH]}\left(\frac{2k_d[I]}{k_t}\right)^{1/2} = \frac{[M]}{[PH]}\left(\frac{2k_d[I]k_i'^2}{k_tk_p^2}\right)^{1/2} \tag{17}$$

Substituting in eq. (13),

$$\frac{d[PM]}{dt} = [M]\left(\frac{2k_dk_i'^2[I]}{k_t}\right)^{1/2} \tag{18}$$

On the basis of the equations proposed for our model for each mole of reacted M [step (7)], 1 mol PM is formed [step (8)]. Therefore, the moles of PM formed at time $t$ are given by

$$[PM] = [M]_0 - [M] \tag{19}$$

Moreover, the peroxide concentration at time $t$ is given by

$$[I] = [I]_0e^{-k_dt} \tag{20}$$

$$\frac{d[PM]}{dt} = -\frac{d[M]}{dt} = \left(\frac{2k_dk_i'^2[I]_0}{k_t}\right)^{1/2}[M]\cdot e^{-k_d\cdot t/2} \tag{21}$$

Separating the variables and integrating between the limits 0 and t (0 and [PM]),

$$\int_0^{[PM]} \frac{d\{[M]_0 - [PM]\}}{[M]_0 - [PM]} = -\int_0^t \left(\frac{2k_dk_i'^2[I]_0}{k_t}\right)^{1/2}\cdot e^{-k_d\cdot t/2}\,dt \tag{22}$$

$$\ln\frac{[M]_0 - [PM]}{[M]_0} = \frac{2K}{k_d}\cdot[I]_0\cdot(e^{-k_dt/2} - 1) \tag{23}$$

where $K = k_i'(2k_d/k_t)^{1/2}$, and finally

$$[PM] = [M]_0\left(1 - \exp\left\{\frac{2K}{k_d}[I]_0^{1/2}(e^{-k_d\cdot t/2} - 1)\right\}\right) \tag{24}$$

At limiting conditions of time the above equation reduces to

$$t = 0: \quad [PM] = 0 \tag{25a}$$

$$t = \infty: \quad [PM] = [M]_0\{1 - e^{-(2K\cdot[I]_0^{1/2})/k_d}\} \tag{25b}$$

The time derivative of [PM] is given by

$$\frac{d[PM]}{dt} = [M]_0\left\{\exp\left\{\frac{2K}{k_d}[I]_0^{1/2}(e^{-k_d\cdot t/2} - 1)\right\} \times \left\{\frac{2K[I]_0^{1/2}}{k_d}e^{-k_dt/2}\right\}\frac{k_d}{2}\right. \tag{26}$$

which, at limiting conditions of time, yields

$$\left(\frac{d[PM]}{dt}\right)_{t=0} = [M]_0[I]_0^{1/2}\cdot K \tag{27a}$$

$$\left(\frac{d[PM]}{dt}\right)_{t=\infty} = 0 \tag{27b}$$

Thus the model predicts a one half order of reaction for the initial reaction rate with respect to the radical initiator concentration; this prediction has been confirmed experimentally.[6]

Equation (24) can be rewritten in a more compact form:

$$[PM] = C_0\{1 - \exp\{C_1(e^{-C_2\cdot t} - 1)\}\} \tag{28}$$

where $C_0 = [M]_0$; $C_1 = 2K[I]_0^{1/2}/k_d$, $C_2 = k_d/2$.

## COMPARISON WITH EXPERIMENTAL RESULTS

### Kinetics at Varying $[I]_0$

Since there is no possibility of obtaining the kinetic constants of the single reaction steps $k_i$, $k_d$, and $k_t$ from our experimental data, it was decided to use $C_1$ and $C_2$ as adjustable parameters ($C_0$ is equal to $[M]_0$ and is known) and to obtain the theoretical curves by best fitting the experimental data (see Fig. 3). In particular, a computer program was developed by which $C_1$ and $C_2$ were calculated by a trial and error procedure until the best superposition of the theoretical curves with the data could be obtained (Fig. 3).

The superposition has been obtained by shifting the experimental data of the time corresponding to the induction periods, relative to each curve A, B,

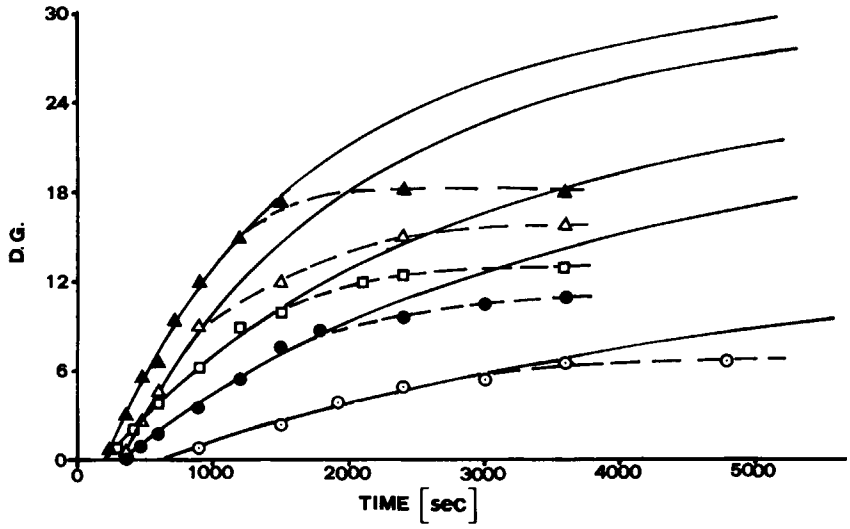


**Figure 3** Comparison between calculated best fitting curves (——) and the experimental data of Figure 1(a): (○, ●, □, △, ▲) compositions A, B, C, D, and E of Table I, respectively.

C, D, and E. This means that such periods represent only a preparation to the starting of DBM grafting. Thus the model can be applied from this time on. Such a procedure presents a problem, which is the actual initial DCPO concentration at time zero (when the induction period comes to an end). At first sight one could say that the actual $[I]_0$ is to be corrected by the amount of $[I]_0$ decomposed before the starting of the DBM grafting reaction. However, the effect of this decomposition is still in the system in that the produced macroradicals are still active so that the grafting reaction can start and go on to a fully developed steady-state regime. Only very few macroradicals are consumed in termination reactions at the beginning of the induction period when the cage effect is very effective.

Moreover, we can assume that the small amount of $[I]_0$ lost in this way is proportional to the same $[I]_0$ and/or negligible in absolute. The fit in Figure 3 between experimental data and theoretical values is quite satisfactory at low $[I]_0$ values for almost the whole curve. As $[I]_0$ increases, the theoretical plateaux at infinite time become larger and larger than the experimental ones. Furthermore, it is evident that the shape of the curves is quite different in the two cases. In fact, the model yields curves whose derivative smoothly increases. The experimental data, however, follow an initial linear trend and then quite abruptly level off, indicating that the reaction has come to completion in a relatively short time. Therefore, the model is suitable to describe only the beginning of the reaction and its steady state portion of the curves (where the trend is rather linear).

In Table I the $C_1$ and $C_2$ values and their product $C_1C_2$ are reported as a function of $[I]_0^{1/2}$, together with the curve codes adopted in Figure 3. The product $C_0C_1C_2$ represents the initial slope at time zero [eq. (27a)]. It is noted that $C_2$ has an average value of $1.86 \times 10^{-4}$ s$^{-1}$ with a minimum of $1.62 \times 10^{-4}$ s$^{-1}$ and a maximum of $1.98 \times 10^{-4}$ s$^{-1}$. Moreover, $C_2$ is practically constant for the first four curves while showing a slight decrease ($1.62 \times 10^{-4}$ s$^{-1}$) only for the curve relative to the highest $[I]_0$.

These results are in agreement with the model

**Table I Values of the Parameters of Eq. (28), $C_1$, $C_2$ and $C_1C_2$ as a Function of $[I]_0^{1/2}$**

| Curve Code | $[I]_0^{1/2}$ (mmol/100 g) | $C_1$ (mmol$^{-1}$ 100 g) | $C_2 \times 10^4$ (s$^{-1}$) | $C_1C_2 \times 10^4$ (mmol$^{-1}$ 100 g s$^{-1}$) |
|---|---|---|---|---|
| A | 1.06 | 0.54 | 1.90 | 1.03 |
| B | 1.26 | 1.23 | 1.92 | 2.36 |
| C | 1.50 | 1.67 | 1.97 | 3.31 |
| D | 1.84 | 3.00 | 1.88 | 5.62 |
| E | 2.12 | 4.16 | 1.62 | 6.75 |

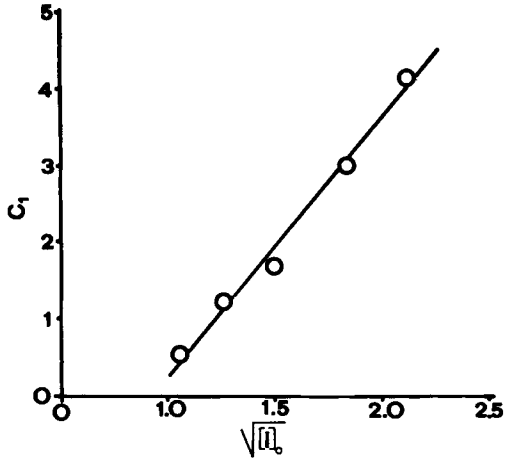


**Figure 4** The values of the $C_1$ parameter of Table I as a function of $[I]_0^{1/2}$.

prediction whereby $C_2 = k_d/2 = \text{const}$ at constant temperature. From the average value of $C_2$, one obtains $k_d/2$, i.e., one half of the kinetic constant of DCPO thermal decomposition at 150°C. Its value ($2.0 \times 10^{-4}\ s^{-1}$) compares quite favorably with that reported in the literature for the DCPO thermal decomposition in aliphatic solvents ($3.0 \times 10^{-4}\ s^{-1}$ [6]).

In Figure 4 the parameter $C_1$ has been plotted as a function of $[I]_0^{1/2}$; a linear correlation is observed in agreement with the theoretical expression of $C_1$: $C_1 = (2K/k_d) \cdot [I]_0^{1/2}$. We have already observed that the only $C_2$ value that presents a deviation with respect to the others is the one relative to curve E. It corresponds to the highest DCPO initial concentration, for which, evidently, the model predictions become less accurate. The reason for this could be ascribed to the fact that, when the concentration of primary radicals R· produced by the DCPO thermal decomposition increases beyond a certain limit, a number of bimolecular coupling reactions, neglected in our model [particularly step (6)], come into play in the reaction mechanism. Furthermore, the coupling, step (3), overcomes scission, step (5). This conclusion is indirectly supported by the anomalous shape of the $[\eta]$ versus time curve, relative to composition E, with respect to the other investigated compositions [see Fig. 1(b)]. The increase of $[\eta]$ at long reaction times observed in the former case clearly indicates in fact a marked change in the overall reaction mechanism governing the process, and an increase in molecular weight.

## Kinetics at Varying Temperature

In Table II the values of $C_1$ and $C_2$, obtained as previously by superimposing the theoretical curves with the experimental data, are reported as a function of the reaction temperature. In Figure 4 the $C_2$ values have been correlated in an Arrhenius plot in the light of the theoretical expression of $C_2$ ($C_2 = k_d/2$). If the model predictions in the investigated temperature range were correct, a linear Arrhenius plot would be the result, with an activation energy of 37 kcal/mol.[5] From Figure 5 it is evident that the expected behavior (dashed straight line) is not observed, indicating a disagreement between the model predictions and the experimental results, particularly at high temperatures (160 and 180°C). The trend at lower temperatures, however, can be reasonably approximated by the expected straight line.

In our opinion the two following factors might be the main reasons for the limits of our model in predicting the kinetic behavior of the system over a relatively wide temperature range:

i. By increasing the temperature, the DCPO decomposition rate increases exponentially, thus producing locally a high concentration of active species. Beyond a certain value of temperature, in such less controlled conditions, some of the termination steps neglected in our reaction scheme may play an increasingly important role.
ii. For the same reasons outlined before (high concentration of active species) it may be dif-

**Table II Values of the Parameters $C_1$, $C_2$, and $C_1C_2$ as a Function of the Reaction Temperature**

| Temperature (°C) | $C_1$ ($mmol^{-1}$ 100 g) | $C_2 \times 10^4$ ($s^{-1}$) | $C_1C_2 \times 10^4$ ($mmol^{-1}$ 100 g $s^{-1}$) |
|---|---|---|---|
| 130 | 2.5 | 0.12 | 0.31 |
| 140 | 0.95 | 1.12 | 1.07 |
| 150 | 1.63 | 1.97 | 3.21 |
| 160 | 3.73 | 2.47 | 9.20 |
| 180 | 15.6 | 3.16 | 49.0 |

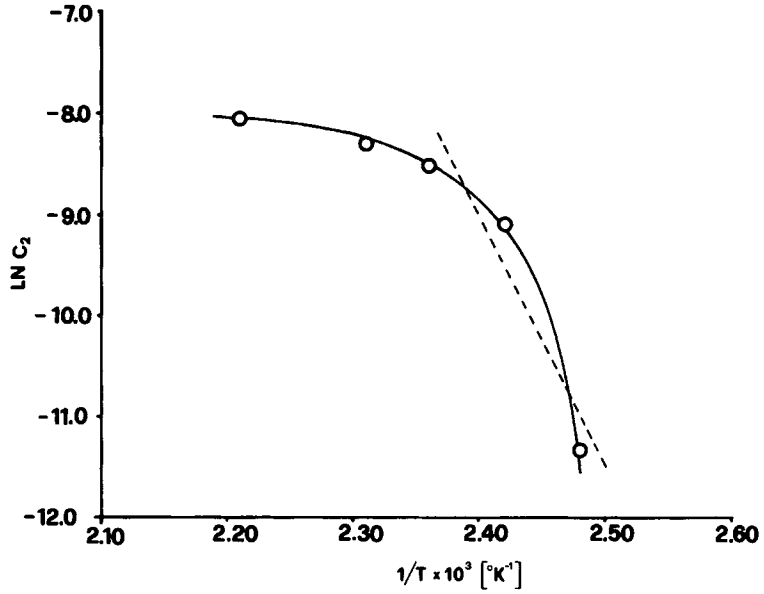


**Figure 5** Arrhenius plot of the parameter $C_2$ of Table II.

ficult or even impossible to reach a steady state condition for the radical species R·, P·, and PM·.

## CONCLUSIONS

A mathematical model for the bulk functionalization of polyolefins has been developed making a number of simplifying assumptions, the most important of which are:

i. A series of bimolecular coupling reactions have been neglected.
ii. A steady state condition has been applied to the radical species R·, P·, and PM·.

Both these conditions require that at any time the radical species concentration is very low and that no accumulation can occur. This can be verified at low rates of decomposition of the radical initiator DCPO. In fact, in such a case, after the induction period, the reactive system reaches a steady state regime and a direct correlation between the grafting reaction of DBM and the molecular degradation can be established. When the DCPO decomposition rate increases, the concentration of radical species become too high to reach a steady-state condition and, furthermore, most of the bimolecular coupling reactions must be taken into account. Therefore, this theoretical approach is to be considered as a limiting model, valid at low temperatures (i.e., low DCPO decomposition rates) or, equivalently, at low DCPO initial concentrations. At higher $T$ and $[I]_0$ values a more complex and probably nonanalytical model is needed.

## REFERENCES

1. G. De Vito, G. Maglio, N. Lanzetta, M. Malinconico, P. Musto, and R. Palumbo. *J. Polym. Sci. Polym. Chem. Ed.*, **22,** 1334 (1984).
2. G. Ruggeri, A. Aglietto, A. Petragnani, and F. Ciardelli, *Eur. Polym. J.*, **19,** 863 (1983).
3. N. G. Gaylord and M. K. Mishra, *J. Polym. Sci. Polym. Lett. Ed.*, **21,** 23 (1983).
4. N. G. Gaylord and M. Metha, *J. Polym. Sci. Polym. Lett. Ed.*, **20,** 481 (1982).
5. R. Greco, G. Maglio, E. Martuscelli, P. Musto, and R. Palumbo, *Polym. Process. Eng.*, **4,** 293 (1986).
6. R. Greco, G. Maglio, and P. Musto, *J. Appl. Polym. Sci.*, **33,** 2513 (1987).
7. R. Greco, G. Maglio, P. Musto, and G. Scarinzi, *J. Appl. Polym. Sci.*, **37,** 777 (1989).
8. R. Greco, P. Musto, F. Riva, and G. Maglio, *J. Appl. Polym. Sci.*, **37,** 789 (1989).
9. R. Greco, P. Musto, G. Maglio, G. Scarinzi, and F. Riva, *Rubber Toughened Plastic,* C. K. Riew, Ed., Adv. Chem. Ser. 222, Am. Chem. Soc., Washington, DC, 1989, p. 359.

*Received July 26, 1990*
*Accepted April 17, 1991*